

Article

# Spacer-Controlled Supramolecular Assemblies of Cu(II) with Bis(2-Hydroxyphenylimine) Ligands. from Monoligand Complexes to Double-Stranded Helicates and Metallomacrocycles<sup>†</sup>

Norman Kelly<sup>1</sup>, Franziska Taube<sup>1</sup>, Kerstin Gloe<sup>1</sup>, Thomas Doert<sup>1</sup>, Wilhelm Seichter<sup>2</sup>, Axel Heine<sup>1</sup>, Jan J. Weigand<sup>1,\*</sup> and Karsten Gloe<sup>1,\*</sup>

<sup>1</sup> Department of Chemistry and Food Chemistry, Technische Universität Dresden, 01062 Dresden, Germany; norman.kelly@gmx.de (N.K.); f.taube@hzdr.de (F.T.); kerstin.gloe@chemie.tu-dresden.de (K.G.); thomas.doert@chemie.tu-dresden.de (T.D.); axelheine@gmx.de (A.H.)

<sup>2</sup> Institute of Organic Chemistry, Technische Universität Bergakademie Freiberg, 09596 Freiberg, Germany; wilhelm.seichter@chemie.tu-freiberg.de

\* Correspondence: karsten.gloe@chemie.tu-dresden.de (K.G.); jan.weigand@tu-dresden.de (J.J.W.); Tel.: +49-351-34357 (K.G.); +49-351-463-42800 (J.J.W.); Fax: +49-351-463-31478 (K.G. & J.J.W.);

<sup>†</sup> Dedicated to Professor Peter Mühl on the occasion of his 85th birthday.

Academic Editor: Helmut Cölfen

Received: 28 August 2016; Accepted: 14 September 2016; Published: 21 September 2016

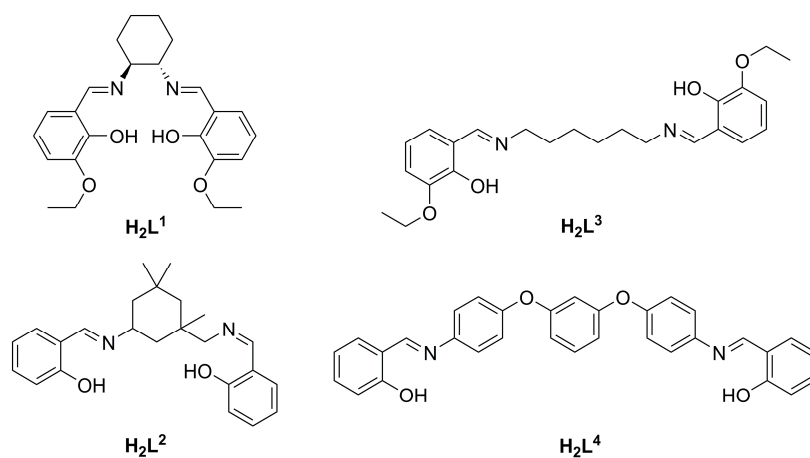
**Abstract:** Reaction of  $\text{Cu}(\text{NO}_3)_2 \cdot 3\text{H}_2\text{O}$  or  $\text{Cu}(\text{CH}_3\text{COO})_2 \cdot \text{H}_2\text{O}$  with the bis(2-hydroxyphenylimine) ligands  $\text{H}_2\text{L}^1$ – $\text{H}_2\text{L}^4$  gave four Cu(II) complexes of composition  $[\text{Cu}_2(\text{L}^1)(\text{NO}_3)_2(\text{H}_2\text{O})] \cdot \text{MeOH}$ ,  $[\text{Cu}_2(\text{L}^2)_2]$ ,  $[\text{Cu}_2(\text{L}^3)_2]$  and  $[\text{Cu}_2(\text{L}^4)_2] \cdot 2\text{MeOH}$ . Depending on the spacer unit, the structures are characterized by a dinuclear arrangement of Cu(II) within one ligand ( $\text{H}_2\text{L}^1$ ), by a double-stranded [2 + 2] helical binding mode ( $\text{H}_2\text{L}^2$  and  $\text{H}_2\text{L}^3$ ) and a [2 + 2] metallomacrocyclic formation ( $\text{H}_2\text{L}^4$ ). In these complexes, the Cu(II) coordination geometries are quite different, varying between common square planar or square pyramidal arrangements, and rather rare pentagonal bipyramidal and tetrahedral geometries. In addition, solution studies of the complex formation using UV/Vis and ESI-MS as well as solvent extraction are reported.

**Keywords:** self-assembly; copper(II); Schiff bases; coordination patterns; helicates; metallomacrocycles

## 1. Introduction

The coordination chemistry of multifunctional Schiff base ligands has been the focus of a considerable number of investigations because they offer application possibilities in catalysis, optics, magnetic materials, sensing, separation, etc. [1–8]. One of the main areas of research relates to the self-assembly of corresponding metal complexes; gaining an understanding of the factors that affect such processes remains a challenge. Among the ligand types studied, tetradentate and hexadentate bis(2-hydroxyphenylimine) ligands are of considerable interest and several examples have been described in the literature [9–12]. Recently, we have published two double-stranded Cu(II) helicates with methylene and sulfurdiphenylene bridged 3-ethoxy-2-hydroxyphenyl substituted diimines. These recognize and bind two water molecules in their peripheral  $\text{O}_4$  cavities [13]. Here we report four further Cu(II) complexes with structure-related hexadentate ( $\text{H}_2\text{L}^1$  and  $\text{H}_2\text{L}^3$ ) and tetradentate diimine ligands ( $\text{H}_2\text{L}^2$  and  $\text{H}_2\text{L}^4$ ) having cyclohexylidene, cyclohexylidenemethylene, hexamethylene and dioxotriphenylene spacer units varying in size and flexibility (Scheme 1). Whereas in case of  $\text{H}_2\text{L}^1$  a dinuclear monoligand Cu(II) complex having an interesting new coordination pattern was formed, for  $\text{H}_2\text{L}^2$  and  $\text{H}_2\text{L}^3$  double-stranded helicates and for  $\text{H}_2\text{L}^4$  a metallomacrocyclic have been isolated

and structurally characterized. The obtained complex structures demonstrate the strong influence of the spacer function on the resulting structure.



**Scheme 1.** Structural formulas of  $\text{H}_2\text{L}^1$ - $\text{H}_2\text{L}^4$ .

## 2. Results and Discussions

### 2.1. Synthesis of the Ligands and Their Cu(II) Complexes

The four diimine ligands  $\text{H}_2\text{L}^1$ - $\text{H}_2\text{L}^4$  have been synthesized by standard Schiff base condensation of salicylaldehyde or 3-ethoxysalicylaldehyde with the different diamines in methanol [14].

Ligand  $\text{H}_2\text{L}^1$  was firstly described by Tozzo et al. [15]. However, in this paper, the elemental analysis is incorrect. The correct data are given here in the Experimental Section. For the introduction of the cyclohexylidene spacer group, the corresponding ( $\pm$ )-*trans*-1,2-diaminocyclohexane was used. A detailed study by Constable et al. using the enantiopure (*R,R*)-cyclohexylidene bridged diimine ligand  $\text{H}_2\text{L}^1$ , showed the formation of two relevant Cu(II) complexes,  $[\text{CuL}^1]$  and  $[(\text{CuL}^1)(\text{H}_2\text{O})]$ , by reaction of  $\text{Cu}(\text{CH}_3\text{COO})_2 \cdot \text{H}_2\text{O}$  and this ligand in methanol [16,17]. Both complexes have a 1:1 (Cu: $\text{L}^1$ ) composition with a square planar Cu(II) arrangement based on the inner  $\text{N}_2\text{O}_2$  donor set. The first of these shows interesting molecular recognition behavior towards a water molecule in the outer  $\text{O}_4$  coordination sphere forming the second complex site. This  $\text{O}_4$  pocket has also been used for the additional binding of s- or f-block metal ions leading to heterodinuclear Cu(II) complexes [17–19]. During our studies, we found that the reaction of the ( $\pm$ )-*trans*-1,2-cyclohexylidene bridged  $\text{H}_2\text{L}^1$  with  $\text{Cu}(\text{NO}_3)_2 \cdot 3\text{H}_2\text{O}$  (molar ratio 1:1) in methanol/tetrahydrofuran (v:v = 1:1) leads to a dinuclear Cu(II) complex. Slow diffusion of diethyl ether/hexane into this solution gave single crystals of composition  $[\text{Cu}_2(\text{L}^1)(\text{NO}_3)_2(\text{H}_2\text{O})] \cdot \text{MeOH}$  that were suitable for X-ray structure determination. However, solids from repeated experiments always gave different analytical results, suggesting the formation of more than one complex species and possibly side products in changing ratios. Besides this 2:1 species (Cu: $\text{L}^1$ ), particularly 1:1 and 2:2 species were each identified in the bulk material by ESI-MS.

$\text{H}_2\text{L}^2$  has been reported by Berkessel et al. [20]. The trimethylcyclohexylidene spacer group in our studies is based on *cis/trans*-5-amino-1,3,3-trimethylcyclohexanemethylamine. Whereas  $\text{H}_2\text{L}^3$  was first described by Ha [21],  $\text{H}_2\text{L}^4$  was synthesized for the first time in this work with this last reaction being catalyzed by addition of a small amount of sulfuric acid.

In contrast to  $\text{H}_2\text{L}^1$  the diimine ligands  $\text{H}_2\text{L}^2$ - $\text{H}_2\text{L}^4$  gave homogeneous dinuclear copper complexes under comparable experimental conditions when reacted with  $\text{Cu}(\text{CH}_3\text{COO})_2 \cdot \text{H}_2\text{O}$  (molar ratio 1:1); namely, the double-stranded helicates  $[\text{Cu}_2(\text{L}^2)_2]$  and  $[\text{Cu}_2(\text{L}^3)_2]$  and the metallomacrocyclic  $[\text{Cu}_2(\text{L}^4)_2] \cdot 2\text{MeOH}$ , respectively. In these cases, single crystals formed on allowing the reaction mixture to stand for one week.

## 2.2. Molecular Structure of the Monoligand Cu(II) Complex with $H_2L^1$

Figure 1 shows the molecular structure of the dinuclear monoligand complex  $[Cu_2(L^1)(NO_3)_2(H_2O)] \cdot MeOH$ . It is crystallized in the triclinic space group  $P-1$ . In this compound both Cu(II) centers show a quite different coordination mode. Cu1 is five-coordinated by the inner square planar  $N_2O_2$  donor set of imine nitrogen atoms and oxygen atoms of deprotonated hydroxyl groups together with one apical nitrate oxygen whereas Cu2 is surrounded by seven oxygen donor atoms involving one deprotonated hydroxyl and one ethoxy group, two bidentate nitrate ions and one water molecule. This results in a distorted square pyramidal arrangement for Cu1 and in a very rare distorted pentagonal bipyramidal coordination geometry for Cu2 [22–26]. The four bond lengths for Cu1-N and Cu1-O in the plane lie in the expected range of strong interactions (Table 1; 1.893–1.951 Å); however, the length of the apical Cu1-O bond (2.658 Å) with the nitrate ion is substantial longer indicating a weak interaction. The seven Cu2-O bond lengths fall within the range 1.951–2.723 Å; stronger interactions with Cu2 occur for the apical water molecule (1.951 Å), the two nitrate ions (1.955 and 2.084 Å) and the hydroxy oxygen donor atom of the ligand (1.987 Å). The remaining Cu2-O interactions with bond lengths of 2.341 Å for the  $C_2H_5O$ -substituent, 2.522 Å and 2.723 Å for the second interactions of both bidentate nitrate ions are all rather weak. Cu1 and Cu2 are directly linked in the structure by two bridging modes, first by strong Cu-O interactions with the hydroxyl oxygen and second by weak Cu-O contacts with one nitrate ion. As a result the distance between both Cu(II) centers is relatively short (3.276 Å). The unique coordination pattern for Cu(II) in the molecule is further stabilized by the water ligand forming two moderate hydrogen bonds  $O1W-H1WB \cdots O1/O2$  with bond lengths of 2.15 Å and 2.05 Å, respectively (Table S1).

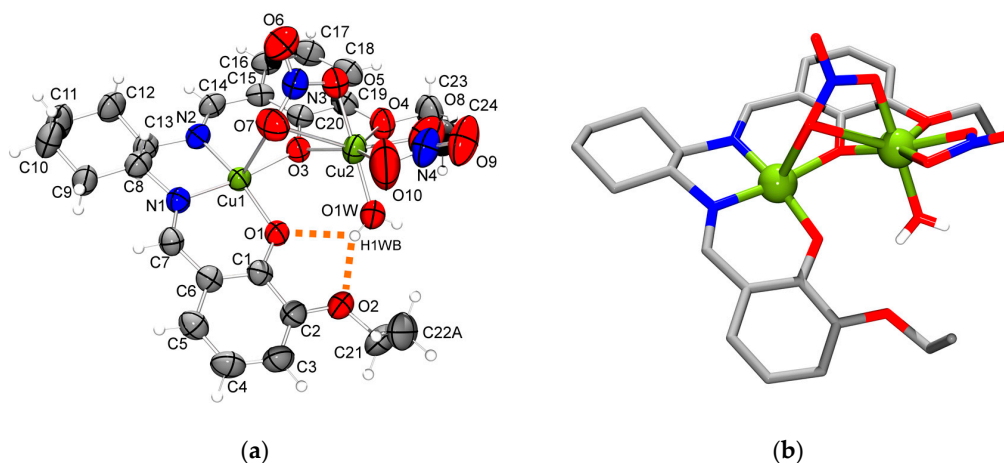


**Figure 1.** ORTEP drawing (50% probability level) of the molecular structure of:  $[Cu_2(L^1)(NO_3)_2(H_2O)] \cdot MeOH$  (a); and simplified stick representation (b).

**Table 1.** Selected bond lengths (Å) in  $[Cu_2(L^1)(NO_3)_2(H_2O)] \cdot MeOH$ .

Bond Lengths			
Cu1-N1	1.926(3)	Cu2-O3	1.987(2)
Cu1-N2	1.951(3)	Cu2-O4	2.341(3)
Cu1-O1	1.893(2)	Cu2-O5	1.955(2)
Cu1-O3	1.951(2)	Cu2-O7	2.723(3)
Cu1-O7	2.658(3)	Cu2-O8	2.084(4)
		Cu2-O10	2.522(7)
		Cu2-O1W	1.951(3)

The coordinated water molecule is also involved in a moderate hydrogen bond  $O1W-H1WA \cdots O9$  (2.11 Å) with a nitrate ion of an adjacent molecule resulting in the formation of

dimeric complex molecules oriented along the crystallographic *c*-axis (Figure 2; Table S2). Each dimer represents a pair of enantiomers introduced in the ligand by the ( $\pm$ )-*trans*-1,2-diaminocyclohexane during the Schiff base synthesis. The dimers are interconnected via weak hydrogen bonds C13-H13 $\cdots$ O3 and  $\pi\cdots\pi$  contacts forming polymeric strands (Tables S2 and S3). Comparable weak hydrogen bonds CH $\cdots$ O and CH $\cdots$  $\pi$  exist between neighboring strands (Figure S1; Tables S2 and S4). The resulting void space in the packing is occupied by strongly disordered methanol molecules. The packing motif is shown in Figure 3 and Figure S2.

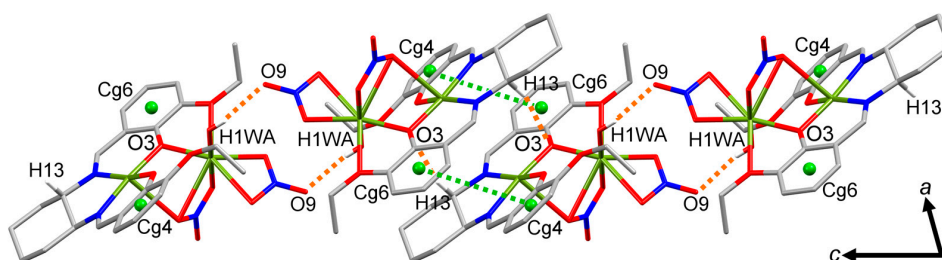


**Figure 2.** Formation of complex dimers and polymeric strands by  $[\text{Cu}_2(\text{L}^1)(\text{NO}_3)_2(\text{H}_2\text{O})]\cdot\text{MeOH}$  via hydrogen bonding and  $\pi\cdots\pi$  interactions.

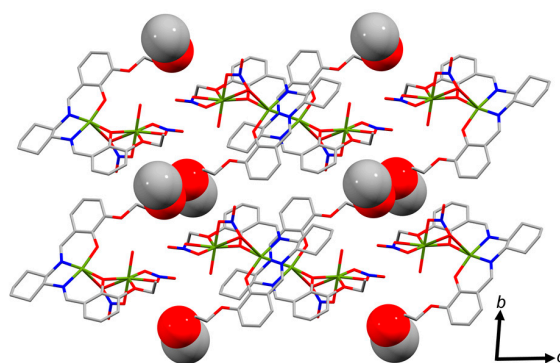


**Figure 3.** Packing of  $[\text{Cu}_2(\text{L}^1)(\text{NO}_3)_2(\text{H}_2\text{O})]\cdot\text{MeOH}$  showing the disordered methanol molecules in the void space.

It is noted that the above Cu(II) complex is structurally comparable to a Zn(II) complex, incorporating the doubly deprotonated form of the related 3-methoxy-2-hydroxyphenylene substituted *cis/trans*-1,2-cyclohexylidene bridged diimine [27]. However, in this case, the coordination number of Zn(II) is five and both Zn(II) centers have a square pyramidal geometry.

### 2.3. Molecular Structure of the Double-Stranded Cu(II) Helicates with $\text{H}_2\text{L}^2$ and $\text{H}_2\text{L}^3$

In contrast to  $\text{H}_2\text{L}^1$  the modified cyclohexylidene spacer function in  $\text{H}_2\text{L}^2$  gives some changes in the latter's size and flexibility. This is clearly reflected in the resulting Cu(II) complex structure (monoclinic space group  $P2_1/c$ ) shown in Figure 4. In this case, Cu(II) forms a neutral dinuclear double-stranded helicate of composition  $[\text{Cu}_2(\text{L}^2)_2]$ . Every helicate unit contains of two deprotonated ligand molecules. Each Cu(II) ion in the complex is coordinated in a strongly distorted square planar arrangement by an  $\text{N}_2\text{O}_2$  donor set. The distortion of the Cu(II) centers is indicated by the parameter  $\tau_4$  [28] which is 0.29 for Cu1 and 0.31 for Cu2. The Cu-O bond lengths are slightly shorter (1.88 Å and 1.89 Å) than the Cu-N bonds (1.99 Å and 2.01 Å; Table 2). Furthermore, the Cu $\cdots$ Cu separation is 5.33 Å and is significantly longer than between the complex molecules (4.13 Å). The presence of weak intramolecular hydrogen bonds C-H $\cdots$ O between  $\text{CH}_2$  groups on the cyclohexane ring and the four oxygen atoms of the hydroxyl groups helps to stabilize the helicate structure (Table S5).

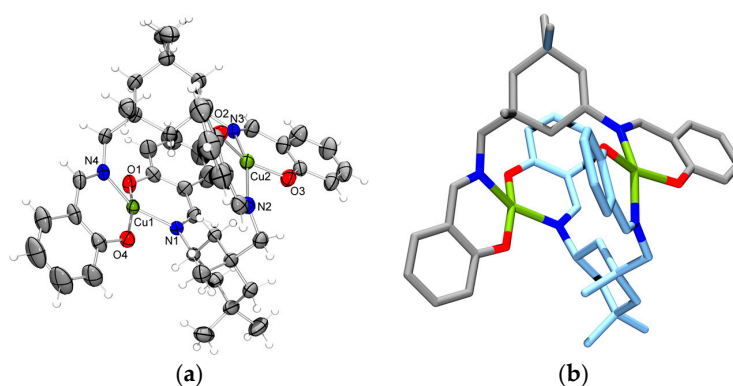


**Figure 4.** ORTEP drawing (50% probability level) of the molecular structure of: [Cu<sub>2</sub>(L<sup>2</sup>)<sub>2</sub>] (a); and a simplified stick representation of the helicate (b).

**Table 2.** Selected bond lengths (Å) in [Cu<sub>2</sub>(L<sup>2</sup>)<sub>2</sub>].

Bond Lengths	
Cu1-N1	2.0065(17)
Cu1-N4	1.9875(19)
Cu1-O1	1.8947(15)
Cu1-O4	1.8828(15)
Cu2-N2	1.9903(19)
Cu2-N3	1.9963(17)
Cu2-O2	1.9007(16)
Cu2-O3	1.8958(17)

Interestingly, only the *cis*-isomers of the ligand have been identified in the crystal structure of [Cu<sub>2</sub>(L<sup>2</sup>)<sub>2</sub>], although both *cis*- and *trans*-isomers were present in the diamine used. Along the crystallographic *c*-axis adjacent helicates are linked by regular stacking of both enantiomers forming polymeric strands. Within these strands, the molecules are connected via CH⋯π and π⋯π interactions (Figure 5 and Figure S3; Tables S6 and S7). In addition, the short distance Cu2⋯Cg10 of 3.90 Å indicates an additional cation⋯π interaction potentially including the imine double bond (Cu2⋯C<sub>imine</sub> = 3.46 Å). Furthermore, within the crystallographic *ac*-plane CH⋯π interactions occur between neighboring strands resulting in the formation of 2D layers. However, no interactions were found between adjacent layers. In contrast to the strands mentioned before, the neighboring helicates possess the same handedness along the crystallographic *a*-axis.

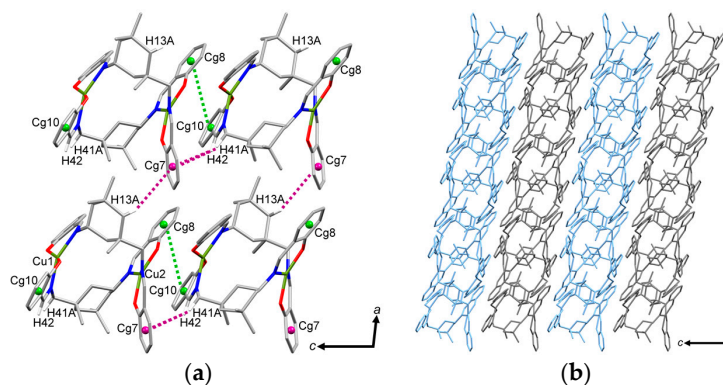


**Figure 5.** Intermolecular CH⋯π and π⋯π interactions in [Cu<sub>2</sub>(L<sup>2</sup>)<sub>2</sub>] resulting in the formation of 2D layers (a); and the resulting packing motif with complex molecules of consistent handedness in the same color (b).

In analogy to  $\text{H}_2\text{L}^2$ , the ligand  $\text{H}_2\text{L}^3$ , possessing a long flexible hexamethylene spacer unit, also reacts with Cu(II) to form a double-stranded helicate of composition  $[\text{Cu}_2(\text{L}^3)_2]$  whose molecular structure (triclinic space group  $P-1$ ) is shown in Figure 6. Both Cu(II) centers possess distorted square planar coordination environments bound to  $\text{N}_2\text{O}_2$  donor sets of two deprotonated ligand molecules ( $\tau_4$ : 0.10 for Cu1; 0.17 for Cu2) [28]. Compared to  $[\text{Cu}_2(\text{L}^2)_2]$ , the Cu-N and Cu-O bond lengths are only slightly different (Table 3). However, in  $[\text{Cu}_2(\text{L}^3)_2]$ , the Cu...Cu separation is 7.09 Å, longer than in  $[\text{Cu}_2(\text{L}^2)_2]$ , while the Cu-Cu distances between adjacent helicates are 5.80 Å and 5.61 Å, respectively. Again, intramolecular hydrogen bonds between  $\text{CH}_2$  groups and nitrogen or oxygen atoms contribute to the stabilization of the helicate (Table S8).

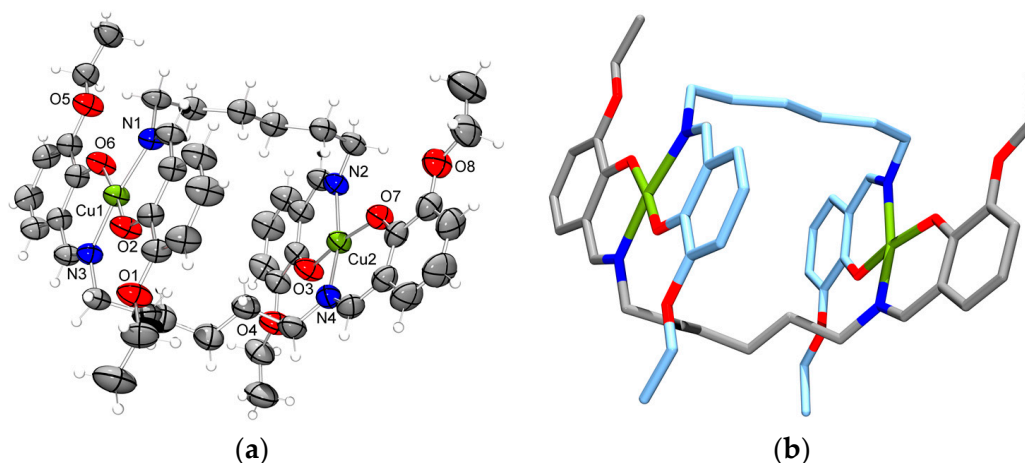


**Figure 6.** ORTEP drawing (50% probability level) of the molecular structure of:  $[\text{Cu}_2(\text{L}^3)_2]$  (a); and stick representation of the helicate (b).

**Table 3.** Selected bond lengths (Å) in  $[\text{Cu}_2(\text{L}^3)_2]$ .

Bond Lengths	
Cu1-N1	2.0022(17)
Cu1-N3	1.9991(17)
Cu1-O2	1.8791(14)
Cu1-O6	1.8722(15)
Cu2-N2	1.9897(19)
Cu2-N4	1.989(2)
Cu2-O3	1.8900(16)
Cu2-O7	1.8838(15)

Remarkably, there are few intermolecular contacts between the complex molecules. Within the crystallographic  $c$ -axis the helicates are linked by  $\text{Cu}\cdots\pi$  interactions to form strand-like arrangements (Figure 7; Table S9). Furthermore, a weak hydrogen bond occurs involving an ethoxy substituent and the oxygen atom O2 (Table S10). The strands contain both left-handed as well as right-handed helices. Due to the long-chain acyclic spacer unit the strands are interlocked forming 2D layers in the  $bc$ -plane (Figure 8).

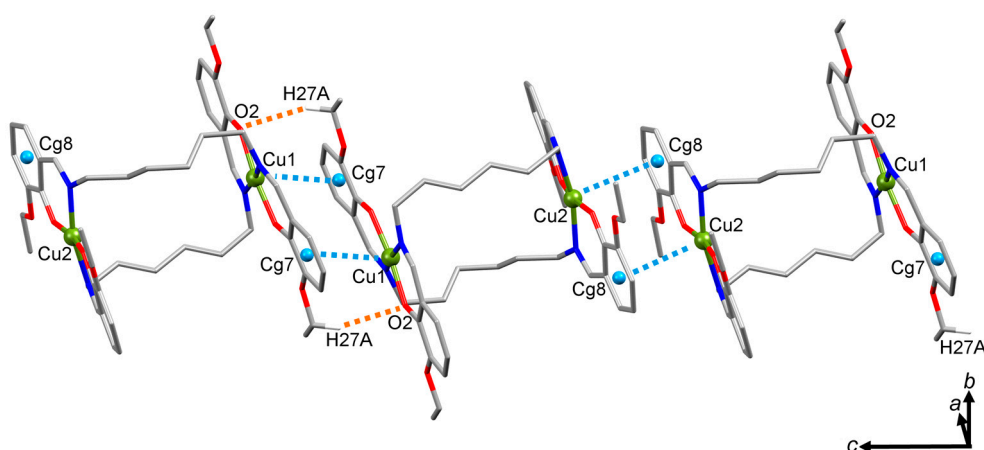


**Figure 7.** Illustration of the formation of polymeric strands by  $[\text{Cu}_2(\text{L}^3)_2]$  involving  $\text{Cu}(\text{II})\cdots\pi$  interactions.

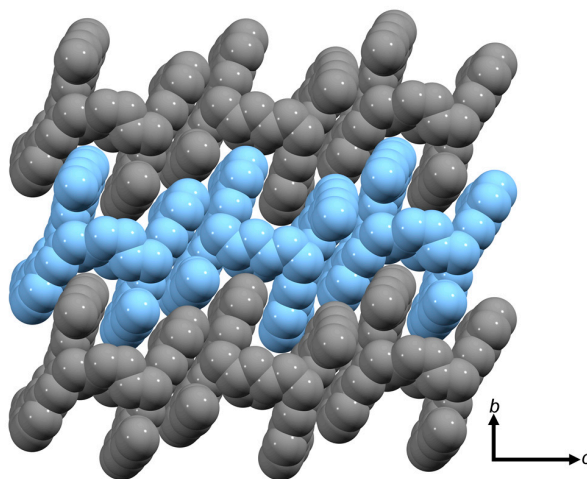


**Figure 8.** 2D layers within the  $bc$ -plane in  $[\text{Cu}_2(\text{L}^3)_2]$ .

#### 2.4. Molecular Structure of the Cu(II) Metallomacrocyclic with $\text{H}_2\text{L}^4$

Ligand  $\text{H}_2\text{L}^4$  is a diimine ligand with a large but limited flexible spacer based on aromatic subunits. In contrast to the other complexes obtained in this study, we were able to isolate a Cu(II) metallomacrocyclic of composition  $[\text{Cu}_2(\text{L}^4)_2]\cdot 2\text{MeOH}$  employing this ligand. Figure 9 shows the molecular structure (monoclinic space group  $P2_1/c$ ) of this compound. The two Cu(II) ions in this dinuclear complex are coordinated in a strongly distorted tetrahedral arrangement ( $\tau_4 = 0.49$ ) [28] by  $\text{N}_2\text{O}_2$  donor sets from two deprotonated ligand molecules. The Cu–O and Cu–N bond lengths are in the expected range and comparable with the three other complexes discussed so far (Table 4). Furthermore, weak  $\text{CH}\cdots\pi$  contacts contribute to the stabilization of the metallomacrocyclic (Table S11). This is in agreement with a structurally related Cu(II) complex discussed by Yoshida et al. [29]. The Cu $\cdots$ Cu separation within the metallomacrocyclic is 16.17 Å and the Cg $\cdots$ Cg distance between the two in 1,3-position bridging central phenylene rings is 6.08 Å. However, this metallomacrocyclic cannot act as a “molecular box” for guest inclusion, because of its flat arrangement. This results from the intramolecular  $\pi\cdots\pi$  interactions between the in 1,4-position bridging aromatic units in the central part of the spacer (Table S12). Therefore any binding of small solvent molecules can only occur in the packing void space, with a methanol molecule bound to an adjacent metallomacrocyclic via moderate bifurcated hydrogen bonds ( $\text{O1A-H1A}\cdots\text{O1}$ , Table S13). However, it is possible to replace methanol by other small solvent molecules like water. This is indicated by the elemental analysis of the bulk material where four water molecules were found instead of two molecules of methanol (Figure S4).

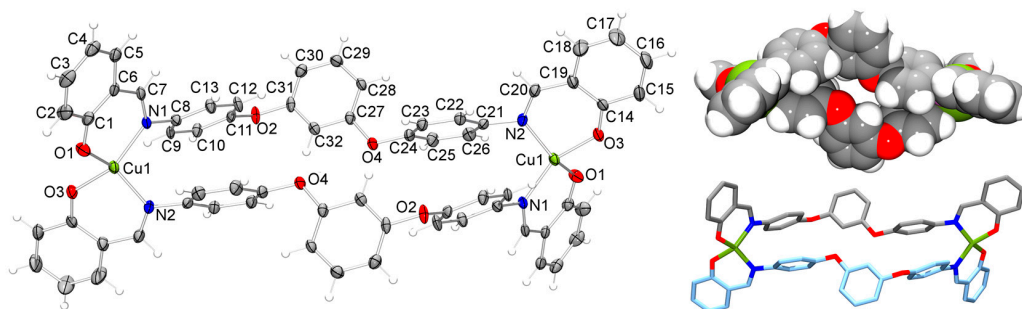


**Figure 9.** ORTEP drawing of the molecular structure of  $[\text{Cu}_2(\text{L}^4)_2] \cdot 2\text{MeOH}$  (Ellipsoids are given at the 50% probability level; disordered  $\text{CH}_3\text{OH}$  is not shown) and the corresponding space fill and capped stick representations.

**Table 4.** Selected bond lengths (Å) in  $[\text{Cu}_2(\text{L}^4)_2] \cdot 2\text{MeOH}$ .

Bond Lengths	
Cu1-N1	1.976(3)
Cu1-N2	1.982(3)
Cu1-O1	1.900(2)
Cu1-O3	1.899(2)

The complex molecules are connected along the crystallographic *a*-axis by hydrogen bonds ( $\text{C10-H10} \cdots \text{O4}$  and  $\text{C23-H23} \cdots \text{O2}$ ; Table S13) and  $\text{CH} \cdots \pi$  contacts ( $\text{C22-H22} \cdots \text{Cg7}$ ; Table S14), in which the central aromatic ring acts as an acceptor (Figure 10). This leads to a regular stacking of the compact metallomacrocycles. The peripheral aromatic units (Cg3) are involved in two  $\pi \cdots \pi$  interactions between adjacent molecules. Additionally, the short  $\text{Cu} \cdots \text{Cg}$  distance of 3.91 Å indicates the presence of a weak metal-aromatic ring contact.

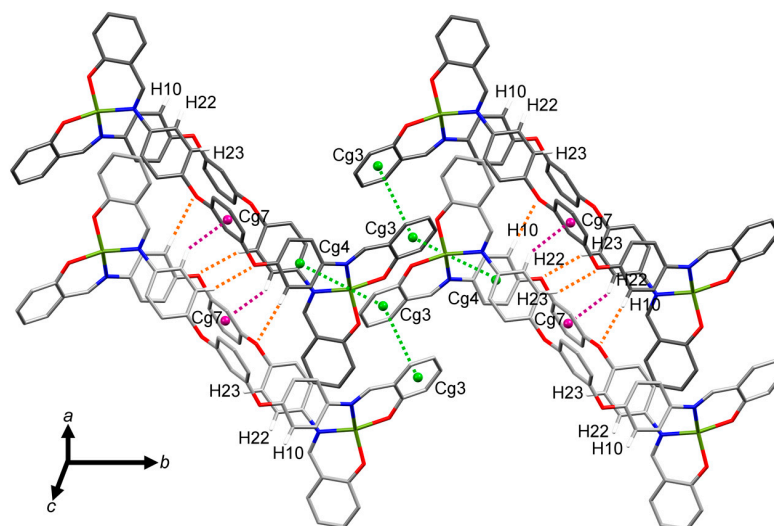


**Figure 10.** Hydrogen bonds,  $\text{CH} \cdots \pi$  and  $\pi \cdots \pi$  interactions between adjacent metallomacrocycles in  $[\text{Cu}_2(\text{L}^4)_2] \cdot 2\text{MeOH}$ .

As shown in Figure 11, the complex molecules possess two different orientations along the crystallographic *c*-axis resulting in a sheet-like assembly. Within the *bc*-plane, the metallomacrocycles are connected via two different hydrogen bonds. Further  $\text{CH} \cdots \pi$  interactions (Table S14) contribute to the organization of this packing motif.

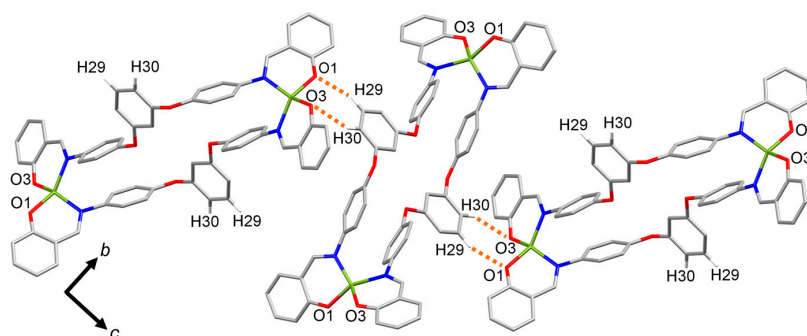


**Figure 11.** Different orientations of the metallomacrocycles in the  $bc$ -plane in  $[\text{Cu}_2(\text{L}^4)_2] \cdot 2\text{MeOH}$ .

### 2.5. UV/Vis Studies of Cu(II) with the Diimines $\text{H}_2\text{L}^1$ – $\text{H}_2\text{L}^4$

A series of UV/Vis spectroscopic studies in combination with electrospray ionization mass spectrometry measurements was performed in order to characterize the complex formation of Cu(II) with the diimine ligands  $\text{H}_2\text{L}^1$ – $\text{H}_2\text{L}^4$  in solution. Figure 12 shows the UV/Vis spectra of  $\text{H}_2\text{L}^1$  in dichloromethane/methanol with changing concentration ratios of Cu(II) and ligand; the constant total concentration was  $3 \times 10^{-3}$  M. The absorption spectrum of  $\text{H}_2\text{L}^1$  exhibits no absorption bands at wavelengths above 520 nm, which is consistent with the yellow color of the ligand solution. The addition of Cu(II) leads to a new band at 560 nm representing the formed Cu(II) complex. The resulting Job plot at this wavelength has a maximum in absorbance for the Cu(II) complexation with  $\text{H}_2\text{L}^1$  at  $x_{\text{Cu(II)}} = 0.5$  and points to a preferred formation of 1:1 complex species between Cu(II) and  $\text{H}_2\text{L}^1$  under the chosen experimental conditions. Furthermore, the absorption spectra show an isosbestic point at 492 nm, which reaches a maximum at  $x_{\text{Cu(II)}} = 0.5$  demonstrating the formation of a 1:1 complex. The ESI-MS spectrum of this sample solution shows a peak at  $m/z = 472.3$  which corresponds to the 1:1 complex species  $[\text{HL} + \text{Cu}]^+$ . Similar results were obtained using Cu(II) nitrate and tetrahydrofuran or dichloromethane/methanol as solvent. Figures S5, S6 and S7 depict the UV/Vis spectroscopic results for complex formation of Cu(II) with  $\text{H}_2\text{L}^2$ – $\text{H}_2\text{L}^4$ , respectively. In all cases, the addition of Cu(II) leads to a new broad shoulder in the wavelength range 400–600 nm. Again, the maximum in absorbance at  $x_{\text{Cu(II)}} = 0.5$  demonstrates the preferred formation of 1:1 complex species. For  $\text{H}_2\text{L}^2$  and  $\text{H}_2\text{L}^3$ , the ESI-MS spectra of a sample solution show peaks corresponding to dinuclear complexes  $([\text{HL} + \text{L} + 2\text{Cu}]^+; m/z = 879.5$  for  $\text{H}_2\text{L}^2$ ,  $m/z = 947.4$  for  $\text{H}_2\text{L}^3$ ). For  $\text{H}_2\text{L}^4$ , the peak at  $m/z = 663.6$  ( $[\text{HL} + \text{Cu}]^+$ ) could also be a result of fragmentation of a dinuclear complex in the gas-phase.

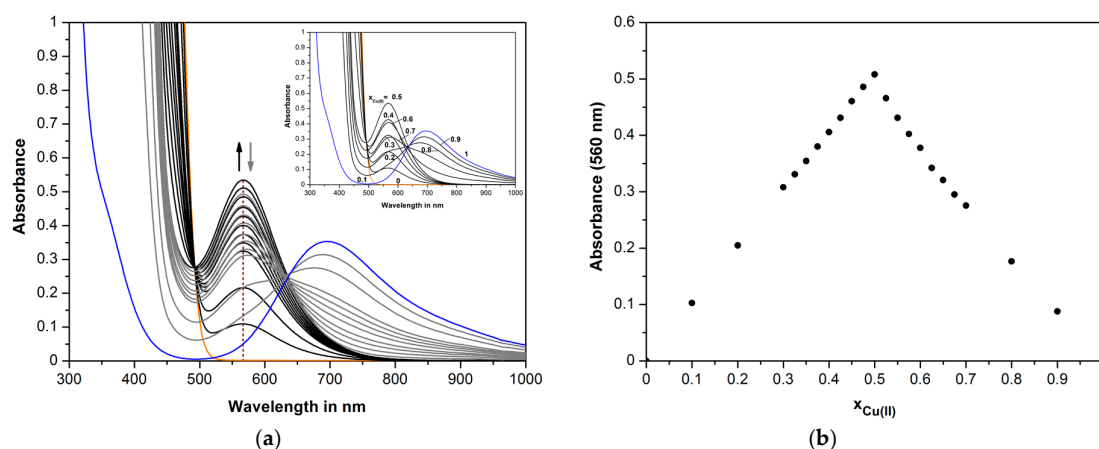


**Figure 12.** UV/Vis spectra (a) and Job plot (560 nm) (b) for the complexation of Cu(II) with  $\text{H}_2\text{L}^1$  in dichloromethane/methanol ( $v/v = 1:1$ );  $[\text{H}_2\text{L}^1] + [\text{Cu(II)}] = 3 \times 10^{-3}$  M ( $x_{\text{Cu(II)}} = 0$ –1),  $t = 30$  min. (copper(II) acetate spectrum in blue, ligand spectrum in orange).

Preliminary liquid-liquid extraction experiments for Cu(II) using the extraction system  $\text{Cu}(\text{NO}_3)_2\text{-NaNO}_3\text{-HEPES buffer-H}_2\text{O}/\text{ligand-CHCl}_3$  were performed for all four ligands (Figure 13). Only the 3-ethoxy-2-hydroxyphenyl substituted ligand  $\text{H}_2\text{L}^3$  extracts Cu(II) quantitatively. However,  $\text{H}_2\text{L}^1$  and  $\text{H}_2\text{L}^4$  also possess a high extraction capability for Cu(II). This result is a proof of sufficient complex stability and lipophilicity of the relevant extracted complexes in solution. Interestingly,  $\text{H}_2\text{L}^2$  shows a significant lower extractability for Cu(II), presumably caused by the complicated steric requirements of the bulky spacer unit affecting the aqueous-organic phase transfer.

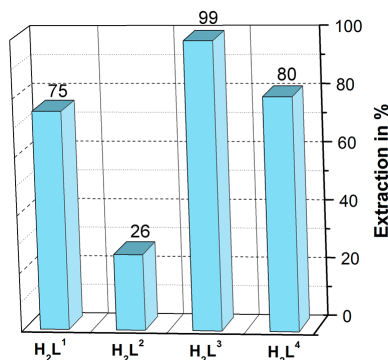


**Figure 13.** Liquid-liquid extraction of Cu(II) by  $\text{H}_2\text{L}^1$ ,  $\text{H}_2\text{L}^2$ ,  $\text{H}_2\text{L}^3$  and  $\text{H}_2\text{L}^4$  at pH = 7.7 (HEPES/NaOH buffer);  $[\text{Cu}(\text{II})] = 1 \times 10^{-4}$  M,  $[\text{NaNO}_3] = 5 \times 10^{-3}$  M;  $[\text{L}] = 1 \times 10^{-3}$  M in  $\text{CHCl}_3$ ;  $t = 30$  min,  $T = 22 \pm 1$  °C.

### 3. Experimental Section

#### 3.1. Reagents and Methodology

All reagents and solvents were purchased from commercial sources and used as received. Elemental analyses were performed with an EA 3000 Euro Vector (HEKATECH, Wegberg, Germany) and a Vario Micro Cube (Elementar, Langensfeld, Germany). The melting points were determined with a Melting Point M-560 (Büchi, Essen, Germany). The NMR spectra were measured with a DRX-500 (Bruker, Karlsruhe, Germany). For UV/Vis studies, a Lambda 25 (PerkinElmer, Rodgau, Germany) spectrophotometer was used. Mass spectra were recorded with an ESQUIRE-detector (Bruker) operated in positive or negative ion electrospray ionization mode.

#### 3.2. X-ray Structure Determinations

Crystals employed for the X-ray determinations were obtained directly from the respective reactions solutions and were used without further drying. Intensities were collected on a Kappa Apex II CCD diffractometer (Bruker AXS) with  $\omega$  and  $\psi$  scans to approximately  $60^\circ$  ( $2\theta_{\text{max}}$ ) at 143(2) or 296(2) K using graphite-monochromated Mo- $\text{K}\alpha$  radiation generated from a sealed tube (0.71073 Å). The Apex Suite [30] program package was used for data collection, integration and data reduction. Multi-scan empirical absorption corrections were applied to all data sets using the program SADABS [31]. The structures were solved by direct methods with the program SHELXS-97 [32] and the full-matrix least squares refinement was performed with SHELXL using the SHELXle user interface [33,34]. In general, ordered non-hydrogen atoms with occupancies greater than or equal to 0.5 were refined anisotropically; partial occupancy solvent oxygen atoms were refined isotropically. Carbon-bound hydrogen atoms were included in idealized positions and refined using a riding model. Oxygen-bound hydrogen atoms that were structurally evident in the difference Fourier map were included and refined with bond length and angle restraints. Parameters for data collection and structure refinement data for all structures are summarized in Table S16. ORTEP [35] depictions of the three structures are given in Figures 1, 4, 6 and 9, selected bond lengths and angles in Tables 1–4 and S1–S15.

CCDC 1488122 ( $[\text{Cu}_2(\text{L}^2)_2]$ ), 1488123 ( $[\text{Cu}_2(\text{L}^3)_2]$ ), 1488124 ( $[\text{Cu}_2(\text{L}^4)_2] \cdot 2\text{MeOH}$ ) and 1488125 ( $[\text{Cu}_2(\text{L}^1)(\text{NO}_3)_2(\text{H}_2\text{O})] \cdot \text{MeOH}$ ) contain the Supplementary Materials crystallographic data for this paper. These data can be obtained free of charge via [www.ccdc.cam.ac.uk](http://www.ccdc.cam.ac.uk), or by contacting The Cambridge Crystallographic Data Centre, 12, Union Road, Cambridge CB21EZ, UK; Fax: +44-1223-336033.

### 3.3. Ligand Syntheses

#### 3.3.1. ( $\pm$ )-*trans*-*N,N'*-Bis(3-ethoxysalicylidene)-1,2-diaminocyclohexane ( $\text{H}_2\text{L}^1$ )

To a solution of ( $\pm$ )-*trans*-diaminocyclohexane (0.57 g, 5.00 mmol) in methanol (20 mL) was added a methanol solution (10 mL) of 3-ethoxysalicylaldehyde (1.66 g, 10.00 mmol). The mixture was stirred for 48 h at room temperature. The solvent was removed under reduced pressure to give a yellow solid residue which was recrystallized from methanol. The solid was washed with methanol and diethyl ether and dried in vacuo. Yellow powder. Yield: 1.80 g (4.40 mmol, 88%). m.p. 125 °C. Calculated for  $\text{C}_{24}\text{H}_{30}\text{N}_2\text{O}_4$  (410.51  $\text{g}\cdot\text{mol}^{-1}$ ): C 70.22; H 7.37; N 6.82. Found: C 69.51; H 7.43; N 7.21. UV/Vis:  $\lambda_{\text{max}}$  (lg  $\epsilon$ ): 221 nm (52398); 259 nm (24885); 327 nm (5510); 414 nm (325). ESI-MS:  $m/z = 411.3$   $[\text{M} + \text{H}]^+$ ; 821.6  $[2\text{M} + \text{H}]^+$ .  $^1\text{H-NMR}$  (500 MHz,  $\text{CDCl}_3$ , 25 °C):  $\delta = 13.90$  (br. s, 2H, OH), 8.22 (s, 2H), 6.84 (dd,  $^3J_{\text{H-H}} = 7.8$  Hz,  $^4J_{\text{H-H}} = 1.4$  Hz, 2H), 6.76 (dd,  $^3J_{\text{H-H}} = 7.8$  Hz,  $^4J_{\text{H-H}} = 1.3$  Hz, 2H), 6.72 (t,  $^3J_{\text{H-H}} = 7.9$  Hz, 2H), 4.06 (q,  $^3J_{\text{H-H}} = 7.0$  Hz, 4H), 3.27–3.29 (m, 2H), 1.85–1.93 (m, 4H), 1.68–1.69 (m, 2H), 1.46 (m, 8H).  $^{13}\text{C-NMR}$  (125 MHz,  $\text{CDCl}_3$ , 25 °C):  $\delta = 164.7$  (2CH), 151.5 (2C<sub>q</sub>), 148.2 (2C<sub>q</sub>), 123.1 (2CH), 118.4 (2C<sub>q</sub>), 117.8 (2CH), 115.0 (2CH), 72.4 (2CH), 64.3 (2CH<sub>2</sub>), 33.0 (2CH<sub>2</sub>), 24.0 (2CH<sub>2</sub>), 14.9 (2CH<sub>3</sub>).

#### 3.3.2. 2-[[5-(2-Hydroxybenzylideneamino)-1,3,3-trimethylcyclohexyl)methylimino]methyl]phenol ( $\text{H}_2\text{L}^2$ )

To a solution of 5-amino-1,3,3-trimethylcyclohexanemethylamine (mixture of *cis* and *trans*; 0.85 g, 5.00 mmol) in methanol (30 mL) was added a methanol solution (20 mL) of salicylaldehyde (1.22 g, 10.00 mmol). The mixture was stirred for 24 h at room temperature. The precipitate was filtered off, washed with methanol and diethyl ether and dried in vacuo. Yellow powder. Yield: 1.05 g (2.77 mmol, 55%). m.p. 141 °C. Calculated for  $\text{C}_{24}\text{H}_{30}\text{N}_2\text{O}_2$  (378.51  $\text{g}\cdot\text{mol}^{-1}$ ): C 76.16; H 7.99; N 7.40. Found: C 76.03; H 7.81; N 7.39. UV/Vis:  $\lambda_{\text{max}}$  (lg  $\epsilon$ ): 256 nm (34733); 317 nm (11885); 407 nm (204). ESI-MS:  $m/z = 379.3$   $[\text{M} + \text{H}]^+$ ; 757.6  $[2\text{M} + \text{H}]^+$ ; 376.9  $[\text{M} - \text{H}]^-$ .  $^1\text{H-NMR}$  (500 MHz,  $\text{CDCl}_3$ , 25 °C):  $\delta = 13.59$  (br. s, 2H, OH), 8.41 (s, 1H), 8.30 (s, 1H), 7.23–7.32 (m, 4H), 6.96 (d,  $^3J_{\text{H-H}} = 8.5$  Hz, 2H), 6.86 (d,  $^3J_{\text{H-H}} = 7.6$  Hz, 2H), 3.57–3.62 (m, 1H), 3.32–3.39 (m, 2H), 1.63 (d,  $^2J_{\text{H-H}} = 12.6$  Hz, 2H), 1.39–1.44 (m, 2H), 1.23–1.26 (m, 2H), 1.20 (s, 3H), 1.11 (s, 3H), 1.00 (s, 3H).  $^{13}\text{C-NMR}$  (125 MHz,  $\text{CDCl}_3$ , 25 °C):  $\delta = 165.4$  (CH), 163.0 (CH), 161.3 (C<sub>q</sub>), 161.2 (C<sub>q</sub>), 132.3 (CH), 131.3 (2CH), 131.2 (CH), 118.7 (2C<sub>q</sub>), 118.54 (2CH), 118.50 (CH), 117.01 (CH), 116.98 (CH), 75.0 (CH<sub>2</sub>), 61.9 (CH), 48.0 (CH<sub>2</sub>), 47.2 (CH<sub>2</sub>), 43.7 (CH<sub>2</sub>), 35.1 (C<sub>q</sub>), 31.5 (C<sub>q</sub>), 28.0 (CH<sub>3</sub>), 24.3 (CH<sub>3</sub>).

#### 3.3.3. *N,N'*-Bis(3-ethoxysalicylidene)-1,6-diaminohexane ( $\text{H}_2\text{L}^3$ )

To a solution of 3-ethoxysalicylaldehyde (1.83 g, 11.00 mmol) in ethanol (40 mL) was added an ethanol solution (20 mL) of hexamethylenediamine (0.58 g, 5.00 mmol). The mixture was stirred for 24 h at room temperature. The precipitate was filtered off, washed with ethanol and diethyl ether and dried in vacuo. Yellow powder. Yield: 1.73 g (4.19 mmol, 84%). m.p. 115 °C. Calculated for  $\text{C}_{24}\text{H}_{32}\text{N}_2\text{O}_4$  (412.52  $\text{g}\cdot\text{mol}^{-1}$ ): C 69.88; H 7.82; N 6.79. Found: C 70.27; H 8.04; N 6.77. UV/Vis:  $\lambda_{\text{max}}$  (lg  $\epsilon$ ): 222 nm (53860); 260 nm (25893); 327 nm (5503); 416 nm (831). ESI-MS:  $m/z = 413.3$   $[\text{M} + \text{H}]^+$ ; 411.0  $[\text{M} - \text{H}]^-$ .  $^1\text{H-NMR}$  (500 MHz,  $\text{CDCl}_3$ , 25 °C):  $\delta = 14.17$  (br. s, 2H, OH), 8.29 (s, 2H), 6.89 (dd,  $^3J_{\text{H-H}} = 7.9$  Hz,  $^4J_{\text{H-H}} = 1.6$  Hz, 2H), 6.84 (dd,  $^3J_{\text{H-H}} = 7.7$  Hz,  $^4J_{\text{H-H}} = 1.4$  Hz, 2H), 6.74 (t,  $^3J_{\text{H-H}} = 7.9$  Hz, 2H), 4.10 (q,  $^3J_{\text{H-H}} = 7.1$  Hz, 4H), 3.58 (m, 4H), 1.66–1.69 (m, 4H), 1.47 (t,  $^3J_{\text{H-H}} = 7.1$  Hz, 6H), 1.41–1.43 (m, 4H).  $^{13}\text{C-NMR}$  (125 MHz,  $\text{CDCl}_3$ , 25 °C):  $\delta = 164.6$  (2CH), 152.7 (2C<sub>q</sub>), 147.8 (2C<sub>q</sub>), 122.8 (2CH), 118.5 (2C<sub>q</sub>), 117.5 (2CH), 115.1 (2CH), 64.4 (2CH<sub>2</sub>), 58.7 (2CH<sub>2</sub>), 30.6 (2CH<sub>2</sub>), 26.7 (2CH<sub>2</sub>), 14.9 (2CH<sub>3</sub>).

### 3.3.4. 1,3-Bis[4-(salicylideneamino)phenoxy]benzol ( $\text{H}_2\text{L}^4$ )

To a suspension of 4,4'-(1,3-phenylenedioxy)dianiline (1.46 g, 5.00 mmol) in methanol (50 mL) was added a methanol solution (10 mL) of salicylaldehyde (1.22 g, 10.00 mmol). Two drops of concentrated sulfuric acid were added and the mixture was refluxed for 8 h. After cooling the precipitate was filtered off, washed with methanol and diethyl ether and dried in vacuo. Pale yellow powder. Yield: 2.18 g (4.36 mmol, 87%). m.p. 131 °C. Calculated for  $\text{C}_{32}\text{H}_{24}\text{N}_2\text{O}_4$  ( $500.54 \text{ g}\cdot\text{mol}^{-1}$ ): C 76.78; H 4.83; N 5.60. Found: C 76.11; H 4.89; N 5.59. UV/Vis:  $\lambda_{\text{max}}$  (lg  $\epsilon$ ): 306 nm (21692); 327 nm (27861); 347 nm (30934). ESI-MS:  $m/z = 501.3$   $[\text{M} + \text{H}]^+$ ; 499.0  $[\text{M} - \text{H}]^-$ .  $^1\text{H-NMR}$  (500 MHz,  $\text{CDCl}_3$ , 25 °C):  $\delta = 13.22$  (br. s, 2H, OH), 8.61 (s, 2H), 7.35–7.39 (m, 4H), 7.31 (s, 1H), 7.27–7.30 (m, 4H), 7.07–7.10 (m, 4H), 7.01 (d,  $^3J_{\text{H-H}} = 7.9 \text{ Hz}$ , 2H), 6.94 (td,  $^3J_{\text{H-H}} = 7.4 \text{ Hz}$ ,  $^4J_{\text{H-H}} = 0.9 \text{ Hz}$ , 2H), 6.77 (dd,  $^3J_{\text{H-H}} = 8.2 \text{ Hz}$ ,  $^4J_{\text{H-H}} = 2.2 \text{ Hz}$ , 2H), 6.72 (t,  $^4J_{\text{H-H}} = 2.2 \text{ Hz}$ , 1H).  $^{13}\text{C-NMR}$  (125 MHz,  $\text{CDCl}_3$ , 25 °C):  $\delta = 161.9$  (2CH), 161.0 (2C<sub>q</sub>), 158.6 (2C<sub>q</sub>), 155.6 (2C<sub>q</sub>), 144.1 (2C<sub>q</sub>), 133.1 (2CH), 132.2 (2CH), 130.6 (1CH), 122.6 (2CH), 120.0 (4CH), 119.2 (2C<sub>q</sub>), 119.1 (2CH), 117.2 (4CH), 113.4 (2CH), 109.3 (1CH).

## 3.4. Complex Syntheses

### 3.4.1. $[\text{Cu}_2(\text{L}^1)(\text{NO}_3)_2(\text{H}_2\text{O})]\cdot\text{MeOH}$

A THF solution of  $\text{H}_2\text{L}^1$  (41 mg, 0.1 mmol, 2 mL) was over-layered with a solution of copper nitrate trihydrate (24 mg, 0.1 mmol, 2 mL) in THF/methanol (v/v = 1:1). Within three days suitable single crystals were obtained by slow diffusion of diethyl ether/hexane (v/v = 1:1). The brown-colored crystals were filtered off, washed with ethanol and diethyl ether and dried in vacuo. Brown crystals. Yield: 23 mg (0.032 mmol, 64%).  $\text{C}_{25}\text{H}_{34}\text{Cu}_2\text{N}_4\text{O}_{12}$  ( $709.66 \text{ g}\cdot\text{mol}^{-1}$ ). ESI-MS:  $m/z = 472.3$   $[\text{HL} + \text{Cu}]^+$ , 943.3  $[\text{HL} + \text{L} + 2\text{Cu}]^+$ , 960.5  $[2\text{L} + 2\text{Cu} + \text{NH}_4]^+$ , 941.4  $[2\text{L} + 2\text{Cu} - \text{H}]^-$ .

### 3.4.2. $[\text{Cu}_2(\text{L}^2)_2]$

Two methanol solutions of  $\text{H}_2\text{L}^2$  (38 mg, 0.1 mmol, 10 mL) and copper acetate monohydrate (20 mg, 0.1 mmol, 10 mL) were combined. After two hours brown-colored plates could be obtained. To complete the precipitation the mixture was left for 24 h. The crystals were filtered off, washed with methanol and diethyl ether and dried in vacuo. Dark brown plates. Yield: 11 mg (0.013 mmol, 25%). Anal. Calcd. for  $\text{C}_{48}\text{H}_{56}\text{Cu}_2\text{N}_4\text{O}_4$  ( $880.07 \text{ g}\cdot\text{mol}^{-1}$ ): C 65.51; H 6.41; N 6.37. Found: C 65.02; H 6.42; N 6.23. ESI-MS:  $m/z = 440.3$   $[\text{HL} + \text{Cu}]^+$ , 879.5  $[\text{HL} + \text{L} + 2\text{Cu}]^+$ .

### 3.4.3. $[\text{Cu}_2(\text{L}^3)_2]$

Two solutions of  $\text{H}_2\text{L}^3$  (41 mg, 0.1 mmol, 50 mL) and copper acetate monohydrate (20 mg, 0.1 mmol, 50 mL) in acetonitrile/methanol (v/v = 1:1) were combined and the mixture was left for one week. Brown crystals could be obtained, which were filtered off, washed with acetonitrile and diethyl ether and dried in vacuo. Brown plates. Yield: 30 mg (0.032 mmol, 63%). Calculated for  $\text{C}_{48}\text{H}_{60}\text{Cu}_2\text{N}_4\text{O}_8$  ( $948.10 \text{ g}\cdot\text{mol}^{-1}$ ): C 60.81; H 6.38; N 5.91. Found: C 60.40; H 6.36; N 5.68. ESI-MS:  $m/z = 474.3$   $[\text{HL} + \text{Cu}]^+$ , 947.4  $[\text{HL} + \text{L} + 2\text{Cu}]^+$ .

### 3.4.4. $[\text{Cu}_2(\text{L}^4)_2]\cdot 4\text{H}_2\text{O}$

Two solutions of  $\text{H}_2\text{L}^4$  (50 mg, 0.1 mmol, 100 mL) and copper acetate monohydrate (20 mg, 0.1 mmol, 100 mL) in dichloromethane/methanol (v/v = 1:1) were combined and the mixture was left for one week. Brown crystals could be obtained, which were filtered off, washed with ethanol and diethyl ether and dried in vacuo. Brown green crystals. Yield: 43 mg (0.035 mmol, 70%). Calculated for  $\text{C}_{65}\text{H}_{56}\text{Cu}_2\text{N}_4\text{O}_{13}$  ( $1228.27 \text{ g}\cdot\text{mol}^{-1}$ ): C 63.56; H 4.60; N 4.56. Found: C 63.79; H 4.14; N 4.28. ESI-MS:  $m/z = 501.3$   $[\text{H}_2\text{L} + \text{H}]^+$ , 663.6  $[\text{HL} + \text{Cu}]^+$ , 661.2  $[\text{L} + \text{Cu} - \text{H}]^-$ .

### 3.5. Liquid-Liquid Extraction

All extraction experiments were performed at room temperature in microcentrifuge tubes (2 mL) by mechanical shaking. The phase ratio  $V_{(w)}:V_{(org)}$  was 1:1 (0.5 mL each); the shaking time was 30 min. The organic phase consists of  $\text{CHCl}_3$  as diluent and the ligand ( $1 \times 10^{-3}$  M). The aqueous phase contained the buffer HEPES/NaOH (pH = 7.7),  $\text{NaNO}_3$  ( $5 \times 10^{-3}$  M) and  $\text{Cu}(\text{NO}_3)_2$  ( $1 \times 10^{-4}$  M). All samples were centrifuged after extraction. The metal concentration in both phases (100  $\mu\text{L}$  samples each) was determined radiometrically using  $\gamma$ -radiation ( $^{64}\text{Cu}$ ; NaI(Tl) scintillation counter Cobra II/Canberra-Packard, Detroit, MI, USA).

## 4. Conclusions

In this study, dinuclear Cu(II) complexes with four diimine ligands were synthesized and characterized in solution and the solid state. The characterized complexes range from a monoligand complex with  $\text{H}_2\text{L}^1$  to [2 + 2] helicates with  $\text{H}_2\text{L}^2$  and  $\text{H}_2\text{L}^3$  and a [2 + 2] metallomacrocyclic complex with  $\text{H}_2\text{L}^4$ . We have demonstrated that the complex structures are strongly influenced by the size and flexibility of the spacer unit. A quite interesting result is the formation of the unique 2:1 (Cu:L) complex by reaction of  $\text{Cu}(\text{NO}_3)_2$  with  $\text{H}_2\text{L}^1$ . This reaction leads to different coordination patterns for the two Cu(II) centers, a commonly observed square pyramidal and a rare pentagonal bipyramidal arrangement. Typically, this ligand forms 1:1 complexes with Cu(II) having a square planar geometry [16,17]. The differences in the literature experimental conditions and our reaction are the counter anion of the Cu(II) salt and the slightly modified solvent system employed; we have used nitrate instead of acetate and the solvent mix methanol/tetrahydrofuran instead of pure methanol.

It is also interesting to note that in contrast to the Cu(II) helicates with the structurally related methylene or sulfurdiphenylene bridged 3-ethoxy-2-hydroxyphenyl substituted diimines [13], the related helicate from  $\text{H}_2\text{L}^3$  having a long hexamethylene spacer cannot bind a water molecule. This is obviously caused by the closely folded structure of this Cu(II) helicate which prevents the preorganization of an outer  $\text{O}_4$  coordination sphere. However, such an environment is able to be generated in the more stretched Cu(II) helicates.

Finally, the UV/Vis and ESI-MS studies performed in dichloromethane/methanol solutions are broadly consistent with the solid state crystallographic results. They also provide some evidence for a preferred formation of dinuclear Cu(II) complex species in solution. However, in the case of  $\text{H}_2\text{L}^1$  the results indicate the presence of several complex species in solution as well as in the solid state. Since the overall reasons for the different behavior of the systems investigated remain unclear, further detailed studies are necessary in order to clarify these results.

**Supplementary Materials:** The following are available online at <http://www.mdpi.com/2073-4352/6/9/120/s1>, Figure S1:  $\text{CH}\cdots\text{O}$  and  $\text{CH}\cdots\pi$  interactions between neighboring strands in  $[\text{Cu}_2(\text{L}^1)(\text{NO}_3)_2(\text{H}_2\text{O})]\cdot\text{MeOH}$ , Figure S2: The packing motif of  $[\text{Cu}_2(\text{L}^1)(\text{NO}_3)_2(\text{H}_2\text{O})]\cdot\text{MeOH}$ , Figure S3: The packing motif of  $[\text{Cu}_2(\text{L}^2)]$ , Figure S4: Methanol molecules in the void space of  $[\text{Cu}_2(\text{L}^4)]\cdot 2\text{MeOH}$  packing, Figure S5: UV/Vis spectra and Job plot for complexation of copper(II) acetate with ligand  $\text{H}_2\text{L}^2$  in THF, Figure S6: UV/Vis spectra and Job plot for complexation of copper(II) acetate with ligand  $\text{H}_2\text{L}^3$  in dichloromethane/methanol, Figure S7: UV/Vis spectra and Job plot for complexation of copper(II) acetate with ligand  $\text{H}_2\text{L}^4$  in dichloromethane/methanol, Table S1: Intramolecular hydrogen bonds in  $[\text{Cu}_2(\text{L}^1)(\text{NO}_3)_2(\text{H}_2\text{O})]\cdot\text{MeOH}$ , Table S2: Intermolecular hydrogen bonds in  $[\text{Cu}_2(\text{L}^1)(\text{NO}_3)_2(\text{H}_2\text{O})]\cdot\text{MeOH}$ , Table S3: Intermolecular  $\pi\cdots\pi$  interactions in  $[\text{Cu}_2(\text{L}^1)(\text{NO}_3)_2(\text{H}_2\text{O})]\cdot\text{MeOH}$ , Table S4: Intermolecular  $\text{CH}\cdots\pi$  interactions in  $[\text{Cu}_2(\text{L}^1)(\text{NO}_3)_2(\text{H}_2\text{O})]\cdot\text{MeOH}$ , Table S5: Intramolecular hydrogen bonds in  $[\text{Cu}_2(\text{L}^2)_2]$ , Table S6: Intermolecular  $\text{CH}\cdots\pi$  interactions in  $[\text{Cu}_2(\text{L}^2)_2]$ , Table S7: Intermolecular  $\pi\cdots\pi$  interactions in  $[\text{Cu}_2(\text{L}^2)_2]$ , Table S8: Intramolecular hydrogen bonds in  $[\text{Cu}_2(\text{L}^3)_2]$ , Table S9: Intermolecular cation $\cdots\pi$  interactions in  $[\text{Cu}_2(\text{L}^3)_2]$ , Table S10: Intermolecular hydrogen bonds in  $[\text{Cu}_2(\text{L}^3)_2]$ , Table S11: Intramolecular  $\text{CH}\cdots\pi$  interactions in  $[\text{Cu}_2(\text{L}^4)_2]\cdot 2\text{MeOH}$ , Table S12: Intramolecular  $\pi\cdots\pi$  interactions in  $[\text{Cu}_2(\text{L}^4)_2]\cdot 2\text{MeOH}$ , Table S13: Intermolecular hydrogen bonds in  $[\text{Cu}_2(\text{L}^4)_2]\cdot 2\text{MeOH}$ , Table S14: Intermolecular  $\text{CH}\cdots\pi$  interactions in  $[\text{Cu}_2(\text{L}^4)_2]\cdot 2\text{MeOH}$ , Table S15: Intermolecular  $\pi\cdots\pi$  interactions in  $[\text{Cu}_2(\text{L}^4)_2]\cdot 2\text{MeOH}$ , Table S16: Crystal and structure refinement data for  $[\text{Cu}_2(\text{L}^1)(\text{NO}_3)_2(\text{H}_2\text{O})]\cdot\text{MeOH}$ ,  $[\text{Cu}_2(\text{L}^2)_2]$ ,  $[\text{Cu}_2(\text{L}^3)_2]$  and  $[\text{Cu}_2(\text{L}^4)_2]\cdot 2\text{MeOH}$ .

**Acknowledgments:** The authors thank the German Federal Ministry of Education and Research (BMBF project 02NUK014A) and the German Federation of Industrial Research Associations (AIF/ZIM project KF2807202RH3) for financial support. Norman Kelly and Franziska Taube thank Margret Acker for assistance in the radiotracer experiments.

**Author Contributions:** Norman Kelly, Kerstin Gloe and Karsten Gloe conceived and designed the experiments; Franziska Taube, Axel Heine and Norman Kelly performed the experiments; Thomas Doert and Willy Seichter were responsible for the single crystal structures; Kerstin Gloe, Karsten Gloe and Jan J. Weigand analyzed the data; and Norman Kelly and Karsten Gloe wrote the paper. All authors discussed the results and commented on the manuscript.

**Conflicts of Interest:** The authors declare no conflict of interest.

## References

1. Yoshida, N.; Oshio, H.; Ito, T. Self-assembling tetranuclear copper(II) complex of a bis-bidentate Schiff base: Double-helical structure induced by aromatic  $\pi\cdots\pi$  and  $\text{CH}\cdots\pi$  interactions. *Chem. Commun.* **1998**, 63–64. [[CrossRef](#)]
2. Yoshida, N.; Oshio, H.; Ito, T. Copper(II)-assisted self-assembly of bis-*N,O*-bidentate Schiff bases: New building blocks for a double-helical supramolecular motif. *J. Chem. Soc. Perkin Trans. 2* **1999**, 975–983. [[CrossRef](#)]
3. Lacroix, P.G. Second-order optical nonlinearities in coordination chemistry: The case of bis(salicylaldiminato)metal Schiff base complexes. *Eur. J. Inorg. Chem.* **2001**, 2001, 339–348. [[CrossRef](#)]
4. Cozzi, P.G. Metal-salen Schiff base complexes in catalysis: Practical aspects. *Chem. Soc. Rev.* **2004**, 33, 410–421. [[CrossRef](#)] [[PubMed](#)]
5. Che, C.-M.; Huang, J.-S. Metal complexes of chiral binaphthyl Schiff-base ligands and their application in stereoselective organic transformations. *Coord. Chem. Rev.* **2003**, 242, 97–113. [[CrossRef](#)]
6. Sakamoto, M.; Manseki, K.; Okawa, H. d-f Heteronuclear complexes: Synthesis, structures and physicochemical aspects. *Coord. Chem. Rev.* **2001**, 219–221, 379–414. [[CrossRef](#)]
7. Whiteoak, C.J.; Salassaa, G.; Kleij, A.W. Recent advances with  $\pi$ -conjugated salen systems. *Chem. Soc. Rev.* **2012**, 41, 622–631. [[CrossRef](#)] [[PubMed](#)]
8. Lacroix, P.G.; Malfant, I.; Real, J.-A.; Rodriguez, V. From magnetic to nonlinear optical switches in spin-crossover complexes. *Eur. J. Inorg. Chem.* **2013**, 2013, 615–627. [[CrossRef](#)]
9. Vigato, P.A.; Tamburini, S. The challenge of cyclic and acyclic Schiff bases and related derivatives. *Coord. Chem. Rev.* **2004**, 248, 1717–2128. [[CrossRef](#)]
10. Vigato, P.A.; Tamburini, S.; Bertolo, L. The development of compartmental macrocyclic Schiff bases and related polyamine derivatives. *Coord. Chem. Rev.* **2007**, 251, 1311–1492. [[CrossRef](#)]
11. Biswas, S.; Ghosh, A. Use of Cu(II)-di-Schiff bases as metalloligands in the formation of complexes with Cu(II), Ni(II) and Zn(II) perchlorate. *Polyhedron* **2013**, 65, 322–331. [[CrossRef](#)]
12. Nathan, L.C.; Koehne, J.E.; Gilmore, J.M.; Hannibal, K.A.; Dewhirst, W.E.; Mai, T.D. The X-ray structures of a series of copper(II) complexes with tetradentate Schiff base ligands derived from salicylaldehyde and polymethylenediamines of varying chain length. *Polyhedron* **2003**, 22, 887–894. [[CrossRef](#)]
13. Kelly, N.; Schulz, J.; Gloe, K.; Doert, T.; Gloe, K.; Wenzel, M.; Acker, M.; Weigand, J.J. Self-assembly of double-stranded copper(II) helicates with 2-ethoxy-2-hydroxyphenyl substituted diimines. Synthesis, molecular structure, and host-guest recognition of  $\text{H}_2\text{O}$ . *Z. Anorg. Allg. Chem.* **2015**, 641, 2215–2221. [[CrossRef](#)]
14. Qin, W.; Long, S.; Panunzio, M.; Biondi, S. Schiff Bases: A short survey on an evergreen chemistry tool. *Molecules* **2013**, 18, 12264–12289. [[CrossRef](#)] [[PubMed](#)]
15. Tozzo, E.; Romera, S.; dos Santos, M.P.; Muraro, M.; de A. Santos, R.H.; Liao, L.M.; Vizotto, L.; Dockal, E.R. Synthesis, spectral studies and X-ray crystal structure of *N,N'*-( $\pm$ )-*trans*-1,2-cyclohexylenebis(3-ethoxysalicylideneamine). *J. Mol. Struct.* **2008**, 876, 210–220. [[CrossRef](#)]
16. Constable, E.C.; Zhang, G.; Housecroft, C.E.; Neuburger, M.; Zampese, J.A. Hierarchical multicomponent assembly utilizing sequential metal-ligand and hydrogen-bonding interactions. *CrystEngComm* **2009**, 11, 657–662. [[CrossRef](#)]

17. Constable, E.C.; Zhang, G.; Housecroft, C.E.; Neuburger, M.; Zampese, J.A. Host-guest chemistry of a chiral Schiff base copper(II) complex: Can chiral information be transferred to the guest cation. *CrystEngComm* **2010**, *12*, 1764–1773. [CrossRef]
18. Koner, R.; Lee, G.-H.; Wang, Y.; Wei, H.-H.; Mohanta, S. Two new diphenoxo-bridged discrete dinuclear Cu<sup>II</sup>Gd<sup>III</sup> compounds with cyclic diimino moieties: Syntheses, structures, and magnetic properties. *Eur. J. Inorg. Chem.* **2005**, *2005*, 1500–1505. [CrossRef]
19. Hazra, S.; Koner, R.; Nayak, M.; Sparkes, H.A.; Howard, J.A.K.; Mohanta, S. Cocrystallized dinuclear-mononuclear Cu<sup>II</sup><sub>3</sub>Na<sup>I</sup> and double-decker-triple-decker Cu<sup>II</sup><sub>5</sub>K<sup>I</sup><sub>3</sub> complexes derived from *N,N'*-ethylenebis(3-ethoxysalicylaldehydeimine). *Cryst. Growth Des.* **2009**, *9*, 3603–3608. [CrossRef]
20. Berkessel, A.; Roland, K.; Schröder, M.; Neudörfl, J.M.; Lex, J. Enantiomerically pure isophorone diamine [3-(aminomethyl)-3,5,5-trimethylcyclohexylamine]: A chiral 1,4-diamine building block made available on large scale. *J. Org. Chem.* **2006**, *71*, 9312–9318. [CrossRef] [PubMed]
21. Ha, K. 6,6'-Diethoxy-2,2'-[hexane-1,6-diylbis(nitrilomethanylylidene)]diphenol. *Acta Cryst.* **2011**, *E67*. [CrossRef] [PubMed]
22. Wester, D.; Palenik, G.J. Pentagonal bipyramidal complexes of nickel(II) and copper(II). The relative importance of ligand geometry vs. crystal field effects. *J. Am. Chem. Soc.* **1974**, *96*, 7565–7566. [CrossRef]
23. Nelson, S.M. Developments in the synthesis and coordination chemistry of macrocyclic Schiff base ligands. *Pure Appl. Chem.* **1980**, *52*, 2461–2476. [CrossRef]
24. Drew, M.G.B.; Nelson, J.; Nelson, S.M. Synthesis of some pentagonal-bipyramidal complexes of manganese(II), iron(II), cobalt(II), nickel(II), copper(II), and zinc(II) with a heptadentate Schiff-base ligand and the crystal and molecular structures of a copper(II) complex. *Dalton Trans.* **1981**, 1685–1690. [CrossRef]
25. Sakurai, T.; Kobayashi, K.; Tsuboyama, S.; Konyo, Y.; Nagao, A.; Ishizu, K. Structure of dichloro(5,6,8,9,11,12,14,15-octahydro-2,3-benzo-1,4,7,10,13-pentaoxacyclopentadec-2-ene) copper(II) chloroform solvate, a Cu(II) crown ether complex with pentagonal-bipyramidal geometry. *Acta Cryst.* **1983**, *C39*, 206–208.
26. Diouf, O.; Gaye, M.; Sail, A.S.; Tamboura, F.; Barry, A.H.; Jouini, T. Crystal structure of diaqua-2,6-diacetylpyridine-bis(acetylhydrazone)copper(II) complex dinitrate hydrate. *Z. Kristallogr. NCS* **2001**, *216*, 421–422.
27. Zhang, Y.; Feng, W.; Liu, H.; Zhang, Z.; Lü, X.; Song, J.; Fan, D.; Wong, W.-K.; Jones, R.A. Photo-luminescent hetero-trinuclear Zn<sub>2</sub>Ln (Ln = Nd, Yb, Er or Gd) complexes based on the binuclear Zn<sub>2</sub>L precursor. *Inorg. Chem. Commun.* **2012**, *24*, 148–152. [CrossRef]
28. Yang, L.; Powell, D.R.; Houser, R.P. Structural variation in copper(I) complexes with pyridylmethylamide ligands: structural analysis with a new four-coordinate geometry index,  $\tau_4$ . *Dalton Trans.* **2007**, 955–964. [CrossRef] [PubMed]
29. Yoshida, N.; Oshio, H.; Ito, T. Supramolecular motifs in metal complexes of Schiff bases. Part 6.1 Topology of two types of self-assembly of bis-*N,O*-bidentate Schiff base ligands by copper(II) ions. *J. Chem. Soc. Perkin Trans.* **2001**, 1674–1678. [CrossRef]
30. Bruker. *Apex Suite (V. 2012.4)*; Bruker AXS Inc.: Madison, WI, USA, 2012.
31. Sheldrick, G.M. *Bruker AXS Area Detector Scaling and Absorption Correction*; University of Göttingen: Göttingen, Germany, 2008.
32. Sheldrick, G.M. *SHELXS-97, Program for the Solution of Crystal Structures*; University of Göttingen: Göttingen, Germany, 1997.
33. Sheldrick, G.M. A short history of SHELX. *Acta Cryst.* **2008**, *A64*, 112–122. [CrossRef] [PubMed]
34. Hübschle, C.B.; Sheldrick, G.M.; Dittrich, B. ShelXle: A Qt graphical user interface for SHELXL. *J. Appl. Cryst.* **2011**, *44*, 1281–1284. [CrossRef] [PubMed]
35. Farrugia, L.J. ORTEP-3 for Windows—a version of ORTEP-III with a Graphical User Interface (GUI). *J. Appl. Cryst.* **1997**, *30*, 565–566. [CrossRef]

